2012

New Isomers in the Full Seniority Scheme of Neutron-Rich Lead Isotopes: The Role of Effective Three-Body Forces

PHYSICAL REVIEW LETTERS, COLLEGE PK, v. 109, n. 16, supl. 1, Part 1, pp. 2561-2566, OCT 16, 2012
http://www.producao.usp.br/handle/BDPI/37139

New Isomers in the Full Seniority Scheme of Neutron-Rich Lead Isotopes: The Role of Effective Three-Body Forces

A. Gottardo,[1,2,*] J. J. Valiente-Dobón,[1] G. Benzoni,[3] R. Nicolini,[3,4] A. Gadea,[5] S. Lunardi,[2,6] P. Boutachkov,[7] A. M. Bruce,[8] M. Górska,[7] J. Grebosz,[9] S. Pietri,[7] Zs. Podolyák,[10] M. Pfützner,[11] P. H. Regan,[10] H. Weick,[7] J. Alcántara Núñez,[12] A. Algora,[5] N. Al-Dahan,[10] G. de Angelis,[1] Y. Ayyad,[12] N. Alkhomashi,[13] P. R. P. Allegro,[14] D. Bazzacco,[6] J. Benlliure,[12] M. Bowry,[10] A. Bracco,[3,4] M. Bunce,[8] F. Camera,[3,4] E. Casarejos,[15] M. L. Cortes,[7] F. C. L. Crespi,[3] A. Corsi,[3,4] A. M. Denis Bacelar,[8] A. Y. Deo,[10] C. Domingo-Pardo,[7] M. Doncel,[16] Zs. Dombradi,[17] T. Engert,[7] K. Eppinger,[18] G. F. Farrelly,[10] F. Farinon,[7] E. Farnea,[6] H. Geissel,[7] J. Gerl,[7] N. Goel,[7] E. Gregor,[7] T. Habermann,[7] R. Hoischen,[7,19] R. Janik,[20] S. Klupp,[18] I. Kojouharov,[7] N. Kurz,[7] S. M. Lenzi,[2,6] S. Leoni,[3,4] S. Mandal,[21] R. Menegazzo,[6] D. Mengoni,[6] B. Million,[3] A. I. Morales,[3] D. R. Napoli,[1] F. Naqvi,[7,22] C. Nociforo,[7] A. Prochazka,[7] W. Prokopowicz,[7] F. Recchia,[6] R. V. Ribas,[14] M. W. Reed,[10] D. Rudolph,[19] E. Sahin,[1] H. Schaffner,[7] A. Sharma,[7] B. Sitar,[20] D. Siwal,[21] K. Steiger,[18] P. Strmen,[20] T. P. D. Swan,[10] I. Szarka,[20] C. A. Ur,[6] P. M. Walker,[10,23] O. Wieland,[3] H-J. Wollersheim,[7] F. Nowacki,[24] E. Maglione,[2,6] and A. P. Zuker[24]

[1]*Istituto Nazionale di Fisica Nucleare, Laboratori Nazionali di Legnaro, Legnaro I-35020, Italy*
[2]*Dipartimento di Fisica dell'Università degli Studi di Padova, Padova I-35131, Italy*
[3]*Istituto Nazionale di Fisica Nucleare, Sezione di Milano, Milano I-20133, Italy*
[4]*Dipartimento di Fisica dell'Università degli Studi di Milano, Milano I-20133, Italy*
[5]*Instituto de Física Corpuscular, CSIC-Universitat de València, València E-46980, Spain*
[6]*Istituto Nazionale di Fisica Nucleare, Sezione di Padova, Padova I-35131, Italy*
[7]*GSI Helmholtzzentrum für Schwerionenforschung, Darmstadt D-64291, Germany*
[8]*School of Computing, Engineering and Mathematics, University of Brighton, Brighton BN2 4GJ, United Kingdom*
[9]*Niewodniczanski Institute of Nuclear Physics, Polish Academy of Science, Krakow PL-31-342, Poland*
[10]*Department of Physics, University of Surrey, Guildford GU2 7XH, United Kingdom*
[11]*Faculty of Physics, University of Warsaw, Warsaw PL-00681, Poland*
[12]*Universidade de Santiago de Compostela, Santiago de Compostela E-175706, Spain*
[13]*KACST, Riyadh 11442, Saudi Arabia*
[14]*Instituto de Fisica, Universidade de São Paulo, São Paulo 05315-970, Brazil*
[15]*EEI, Universidade de Vigo, Vigo E-36310, Spain*
[16]*Grupo de Física Nuclear, Universidad de Salamanca, Salamanca E-37008, Spain*
[17]*Institute of Nuclear Research of the Hungarian Academy of Sciences, Debrecen H-4001, Hungary*
[18]*Physik Department, Technische Universität München, Garching D-85748, Germany*
[19]*Department of Physics, Lund University, Lund S-22100, Sweden*
[20]*Faculty of Mathematics and Physics, Comenius University, Bratislava 84215, Slovakia*
[21]*Department of Physics and Astrophysics, University of Delhi, Delhi 110007, India*
[22]*Institut für Kernphysik, Universität zu Köln, Köln D-50937, Germany*
[23]*CERN, Geneva CH-1211, Switzerland*
[24]*Université de Strasbourg, IPHC, CNRS, UMR7178, 23 rue du Loess, 67037 Strasbourg, France*

(Received 9 February 2012; revised manuscript received 26 July 2012; published 16 October 2012)

The neutron-rich lead isotopes, up to ^{216}Pb, have been studied for the first time, exploiting the fragmentation of a primary uranium beam at the FRS-RISING setup at GSI. The observed isomeric states exhibit electromagnetic transition strengths which deviate from state-of-the-art shell-model calculations. It is shown that their complete description demands the introduction of effective three-body interactions and two-body transition operators in the conventional neutron valence space beyond ^{208}Pb.

DOI: 10.1103/PhysRevLett.109.162502 PACS numbers: 23.35.+g, 23.20.−g, 21.10.Tg, 21.60.Cs

The shell model is nowadays able to provide a comprehensive view of the atomic nucleus [1]. It is a many-body theoretical framework, successful in explaining various features of the structure of nuclei, based on the definition of a restricted valence space where a suitable Hamiltonian can be diagonalized. This effective interaction originates from realistic two-body nuclear forces based on phenomenological nucleon-nucleon potentials, renormalized to be adapted to the truncated model space. Although the renormalization process can be treated in a rigorous mathematical way, the appearance of effective terms is often neglected in calculations, as a common but incorrect practice. The presence and relevance of these effective forces is well known also in other fields of physics, as for example in condensed matter studies [2]. Indeed, effective three-body terms appear already at the lower perturbation order [3]:

they are relevant for quantitative agreement with the spectroscopic structure of nuclei [4], depending on the specific physics of the system. They should not be conflated with the real three-body forces that affect the monopole properties (shell formation and binding energies) of the nuclear Hamiltonian [5–7]. Effective many-body terms have been largely ignored so far, mainly because spaces involving one major oscillator shell couple directly only to $2\hbar\omega$ excitations, which lead predominantly to two-body effective forces and constant effective charges for the one-body transition operators. Starting from the Ni isotopes, the $0\hbar\omega$ quadrupole coupling to the 2^+ core level becomes crucial but nowadays can be treated by diagonalization of a large space, which avoids the explicit introduction of three-body terms. For heavier nuclei a full calculation is problematic, and the restriction of the valence space may require the introduction of effective three-body potentials and the corresponding need to use two-body electromagnetic transition operators. For example, in the light Sn isotopes the calculations that have been performed to date do not include the full coupling [8,9]. The neutron-rich lead nuclei, with valence neutrons outside the well-established doubly magic core ^{208}Pb, represent an ideal case to study the effects related to the effective three-body forces, as large calculations are feasible and the seniority scheme provides useful guidance. However, this region of the nuclear chart has been traditionally difficult to access experimentally due to its neutron richness and low cross sections, but recent fundamental improvements in experimental techniques have enabled its exploration.

In this Letter, the first spectroscopic results are reported on a number of neutron-rich Pb isotopes with $N > 126$, populated via the fragmentation of a high-energy primary uranium beam. It will be shown how their description requires the introduction of effective three-body interactions and two-body transition operators, questioning the common paradigm of one-body transition operators with constant effective charges to account for the truncated model space.

The following results have been obtained by exploiting the uniqueness of the FRS-RISING setup [10–13] and the UNILAC-SIS accelerator facilities at GSI by using a 1 GeV A ^{238}U beam at an intensity of around 1.5×10^9 ions/spill. The $\sim$1 s spills were separated by $\sim$2 s without beam. The beam impinged on a 2.5 g/cm^2 Be target (followed by a 223 mg/cm^2 Nb stripper) and the isotopes resulting from the fragmentation reaction were separated and identified with the double-stage magnetic spectrometer fragment separator (FRS) [10]. The FRS allows one to discriminate the magnetic rigidities of the fragments with a resolution sufficient to distinguish the masses of adjacent isotopes even at the high masses of interest ($A \sim$ 210–220). In this specific measurement, a significant experimental challenge was the fact that the magnetic rigidities of the primary beam charge states (mainly $^{238}U^{91+}$ and $^{238}U^{90+}$) are similar to the magnetic rigidities of the fully stripped neutron-rich lead isotopes, in particular ^{212}Pb and ^{214}Pb. The high yield of uranium ions from the primary beam would lead to an unacceptably high counting rate in the detectors at the intermediate focal plane, before the Al wedge-shaped degrader. In order to avoid the problem, a homogenous 2 g/cm^2 Al degrader was placed after the first dipole, to exclude from the acceptance of the FRS the uranium charge states, enabling a sustainable counting rate in the intermediate focal plane detectors. Slits after the first and the second dipoles were also partially inserted in the beam line of the spectrometer to cut the remaining contamination from the primary beam charge states and from heavy fragments around the element radium ($Z = 88$). The angle of the wedge-shaped 758 mg/cm^2 Al degrader at the intermediate focal plane was set to produce a monochromatic beam. The identification in mass over charge (A/q) is achieved through time of flight and focal-plane position measurements, while the atomic number is obtained from two ionization chambers placed in the final focal plane. Finally, the comparison of the magnetic rigidities before and after the Al wedge-shaped degrader allows one to discriminate a possible change in the ion charge state. These measurements are sufficient to provide a complete identification of the isotopes event by event.

At the final focal plane, the ions were slowed down in a thick Al degrader in order to reduce the energy of the fragments of interest so they could be implanted in a composite double-sided silicon-strip detector (DSSSD) system comprising 3 layers, each with three DSSSD pads [13,14]. Each DSSSD, 16×16 pixels, had dimensions 5×5 cm^2 and a thickness of 1 mm with an energy detection threshold of 160 keV. The DSSSD system was surrounded by the RISING γ spectrometer [11,12], consisting of 105 germanium crystals arranged in 15 clusters with 7 crystals each. The full-energy gamma-ray peak detection efficiency of the array was measured to be 15% at 662 keV [11] and its time correlation with the active stopper allowed the performance of both isomer spectroscopy and β-delayed γ-ray spectroscopy.

Figure 1 shows the γ-ray spectra following the isomeric decays of ^{212}Pb, ^{214}Pb and ^{216}Pb. The γ spectrum obtained for ^{212}Pb can be compared with the results presented in Ref. [15] where only two transitions could be identified due to statistical limitations, and no level scheme was derived. No information was available on $^{214-216}$Pb, whose levels are observed in this work for the first time. The γ-ray transitions in each of the three cases (^{212,214,216}Pb) are in mutual coincidence and of comparable intensities and decay times. The combination of this experimental information with the expected systematics of even-even nuclei outside a shell closure allows one to firmly establish the level schemes in Fig. 2, where the observed isomers are all interpreted to have spin or parity 8^+ (assuming a predominant, maximally aligned neutron $(g_{9/2})^2$ configuration). The detected γ rays shown in Fig. 1 are then attributed to the $6^+ \rightarrow 4^+ \rightarrow 2^+ \rightarrow 0^+$ yrast cascade. The $8^+ \rightarrow 6^+$ transition is not detected in any of the three cases. This is

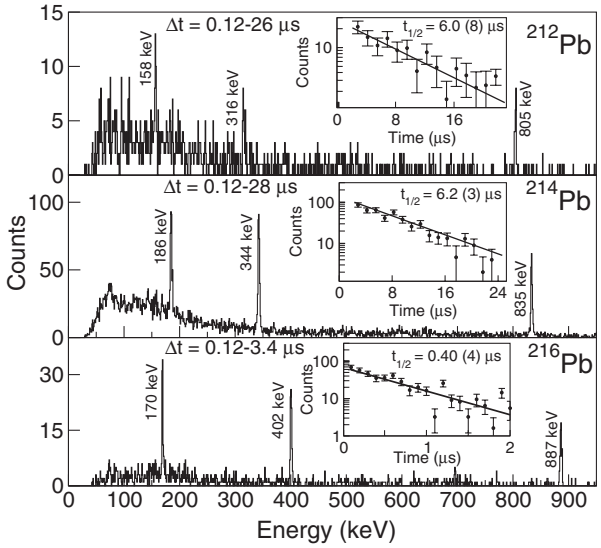

FIG. 1. Time-gated spectra for the isomers observed in ^{212}Pb, ^{214}Pb and in ^{216}Pb. The insets show the decay curve of the isomers.

due to the low energy of this γ-ray transition which is expected to have a significant electron conversion branch competing with the γ-ray emission. The energy of the $8^+ \rightarrow 6^+$ transition in ^{212}Pb is taken from Ref. [16], while the same transition in ^{214}Pb and in ^{216}Pb is assumed to be between 20 and 90 keV. The characteristic K_α x rays from lead at 75 keV are observed with an intensity compatible with their origin only from the internal conversion of the $6^+ \rightarrow 4^+$ transition. Therefore, it is inferred that the $8^+ \rightarrow 6^+$ energy must be below the 88 keV binding energy of the lead K electrons, and hence the given upper limit. From systematics, a conservative lower limit of 20 keV is adopted. The isomer lifetimes have been determined by exponential fits to the decay curves. Although the energy of the 8^+ state is not known for ^{214}Pb and ^{216}Pb, the strong

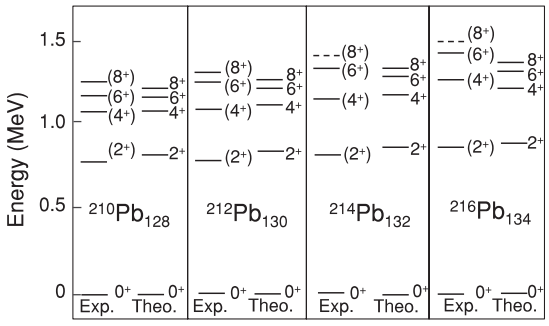

FIG. 2. Deduced level schemes for the even-even neutron-rich lead isotopes (Exp.), compared with $(g_{9/2}i_{11/2}d_{3/2}d_{5/2}g_{7/2}s_{1/2}j_{15/2})^n$ shell-model calculations with the Kuo-Herling interaction (Theo.). ^{210}Pb and the 8^+ state in ^{212}Pb were not observed in the experiment and are reported for completeness. The 8^+ state in ^{214,216}Pb has been drawn at an estimated energy of approximately 60 keV above the observed 6^+ state.

energy dependence of the $E2$ transition rate is compensated by a similar but opposite energy dependence of the total $E2$ conversion coefficient, which makes the extracted $B(E2)$ value only weakly dependent on the transition energy. Therefore, it is possible to provide a reliable estimate of the $B(E2)$ strengths for all of the isomeric decays observed, as shown in Fig. 3. For ^{214,216}Pb, the interval of $B(E2)$ values for the $8^+ \rightarrow 6^+$ transition-energy range 20–90 keV is reported.

The experimental level schemes for $^{210-216}$Pb in Fig. 2—consistent with $g^n_{9/2}$ dominance in a seniority scheme [17,18]—are well described by calculations with the shell-model codes ANTOINE and NATHAN [19,20], using the Kuo-Herling (KH) interaction [21], the experimental spectrum of ^{209}Pb for the single-particle energies, and the pure neutron valence space $(g_{9/2}i_{11/2}d_{3/2}d_{5/2}g_{7/2}s_{1/2}j_{15/2})^n$ beyond the closed ^{208}Pb core. From the same shell-model calculations the reduced-transition probability $B(E2)$ values from the isomeric states were estimated, using an effective charge for neutron $e_\nu = 0.8$, which is consistent with the value usually employed in this space [21]. While the average agreement between experimental and theoretical level energies is very good, within ~100 keV, the situation is quite different for the $B(E2)$ values, which are a sensitive probe of the wave function: see Fig. 3. On one hand, while experimental values seem to roughly follow the parabolic behavior predicted by the seniority scheme, the transition rates in ^{212,214}Pb are overestimated by a factor of two. On the other hand, the more detailed and realistic calculation in the full valence space with the KH interaction (red dashed line) largely overestimates the $B(E2)$ in ^{212}Pb by a factor five and it predicts

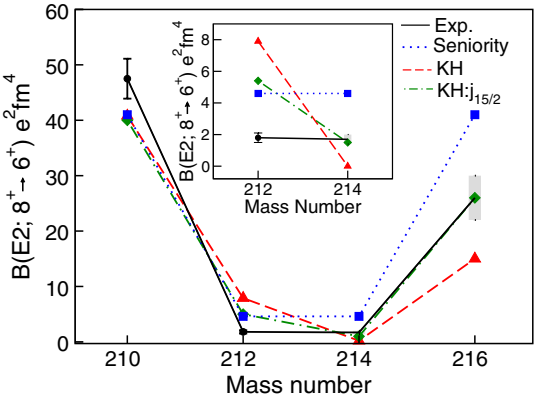

FIG. 3 (color online). Measured $B(E2)$ values for the isomeric states (black continuous line), compared with shell-model calculations in the neutron space beyond ^{208}Pb. For ^{214,216}Pb the range of measured $B(E2)$ values is indicated with a shaded area. The blue dotted line reports the results from the pure seniority scheme in the $g_{9/2}$ shell, the red dashed line represents the full diagonalization in the neutron space with the KH interaction while the green dash-dotted line is the same calculation, but with the energy of the $j_{15/2}$ orbital increased by 1 MeV.

a too low $B(E2)$ for ^{214}Pb. Therefore, the large-scale shell-model calculations not only cannot reproduce the hindrance of the $B(E2)$ values in ^{212}Pb but also introduce an asymmetry around midshell not present in the experimental data. One objection to our calculations could arise from the value of the single particle energy of the $\nu j_{15/2}$ orbital taken from the spectrum of ^{209}Pb, due the presence of a strong mixture of $j_{15/2}$ and $g_{9/2} \otimes 3^-$ [22]. If half of the spectroscopic strength is assumed to be at about 3.5 MeV [23], then the single-particle energy has to be shifted by 1 MeV: the disagreement with the $B(E2)$ rates decreases, though it does not vanish, as shown in Fig. 3 by the green dashed-dotted line. Moreover, other problems arise, such as the tendency of the $B(E2)$ of the 4^+ state in ^{214}Pb to go to zero, thereby creating an isomeric yrast 4^+ state which is not observed experimentally.

Other modern realistic interactions (for example CD-BONN potential [24] in a V_{lowK} approach) give similar discrepancies between theory and experiment. In fact, the overlap between realistic interactions is generally quite high, thereby proving their universal character [1]. Since the results in the $B(E2)$ values of Pb isotopes are somehow interaction independent, the disagreement encountered cannot be explained by problems in the two-body interaction.

In the following it will be shown that the inclusion of the effective three-body forces is essential to understand the observed transition rates. These often ignored terms have not been explicitly treated in a full perturbative calculation so far. However, following the rigorous analysis of Ref. [4], in this work their effects are assessed by explicitly considering the relevant particle-hole (p-h) excitations from the core. It is known that one of the central basic tenets of modern nuclear shell model is the use of a two-body interaction renormalized for the chosen valence space (with monopole corrections which can also account for the effect of real three-body interaction [5]). This renormalization process takes into account excitations from the core and it affects the matrix elements of the Hamiltonian and also the electromagnetic transition operators leading to effective charges for neutrons and protons, which remain constant in the valence space and are the standard $e_\nu = 0.5e$, $e_\pi = 1.5e$ [1]. However, already at the second order (i.e., with p-h excitations from the core) effective three-body forces appear, as well as effective two-body transition operators [4]. Nevertheless, their neglect even in modern large-scale shell model calculations is a common but bad practice. Their effect is here studied by dressing the bare wave function $g^n_{9/2}$ with p-h excitations from closed-core shells [4], as shown by the diagrams in Fig. 4. The resulting excitation matrix elements produce both the famous bubble diagram on the left and its—almost universally neglected—three-body counterpart on the right. The bubble may consist of excitations at 0 or $1\hbar\omega$ (as for the 2^+ and 3^- in ^{208}Pb) or $2\hbar\omega$ (giant quadrupole resonance) that

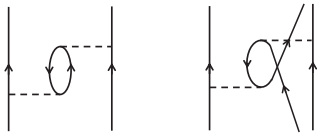

FIG. 4. The bubble diagrams: the open lines correspond to valence orbits. The interaction lines are associated with matrix elements which enable us to go from one configuration to another with particle-hole excitations.

affect all model spaces and lead in particular to constant effective charges. Concerning the coupling to the collective 3^- octupole, it affects the $g^n_{9/2}$ bare wave function only indirectly in higher order perturbation theory. Therefore, only the two-body effective contributions included in the interaction will be taken to represent the octupole coupling. In contrast, the core-excited 2^+ *phonon* couples directly to the dominant $g^n_{9/2}$ configurations in second order through very specific $\Delta j = 2$ particle-hole jumps responsible for quadrupole coherence [[1], p. 463]. Such particle-hole jumps ($h^{-1}_{11/2} f_{7/2}$ for protons and $i^{-1}_{13/2} g_{9/2}$ for neutrons) are equivalent to account for effective three-body forces and effective two-body operators, see Fig. 4 and Ref. [4]. Their effects are important and are estimated using the Kahana Lee Scott (KLS) interaction [25], which is an old realistic potential whose matrix elements are identical to the most modern ones within better than 96% overlaps ([1,25] and references therein). Simple diagonalizations including these jumps are no substitute for a full perturbative treatment but give indications of what could be expected, regarding in particular the restoration of the observed seniority regularities: results are shown in Fig. 5. Effective charges are the standard $1.5e$ and $0.5e$ for protons and neutrons, respectively. The theoretical values for the other states and the sign of the quadrupole moments Q are also given for completeness. Case A (red dashed line) is a diagonalization in the pure $g_{9/2}$ shell, where the seniority scheme is trivially valid, whereas case B (green dot-dashed line) includes p-h excitations to the other neutron shells above the core and should be regarded as a simulation of a full diagonalization of the valence space. From their comparison, a state dependence of the effective charges is evident, appearing as a clear breaking of the midshell symmetry. The inversion of the quadrupole sign in the 4^+, 6^+ states in ^{212,214}Pb with respect to case A is also a striking feature: no simple effective-charge adjustment can account for an inversion of the quadrupole sign. Case C (blue dotted line), where p-h jumps from both the proton and neutron cores are introduced allowing configurations of the type $\pi h^{-1}_{11/2} \pi f_{7/2}$ and $\nu i^{-1}_{13/2} \nu g_{9/2}$, shows the effect of the so far neglected effective three-body forces of Fig. 4 when compared to case B. In the first place, the transition rates nearly double from case B to case C, which corresponds to e_ν going roughly from $0.5e$ to $0.7e$, not far from the $0.8e$ adopted in Fig. 3. Second, the asymmetry around midshell is almost recovered for the experimentally

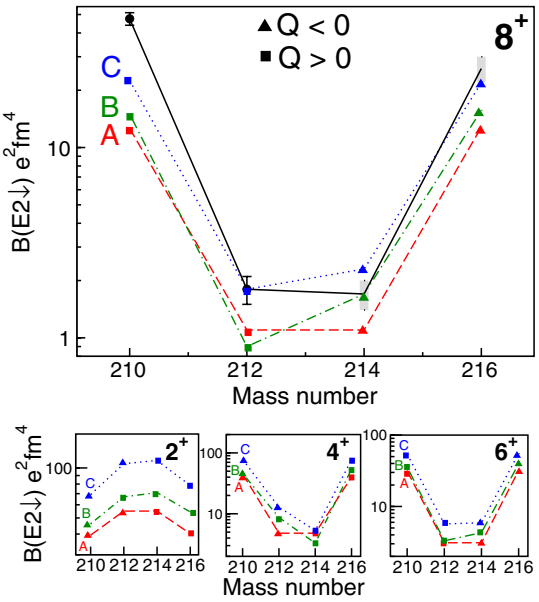

FIG. 5 (color online). Transition rates and sign of the quadrupole moments for the even-even Pb isotopes. Diagonalizations are made in the following spaces: case A in red dashed line $\equiv g^n$; case B in green dot-dashed line $\equiv g^n + g^{n-1}r$; case C in dotted blue line $\equiv g^n + g^{n-1}r + g^n([h_{11/2}^{-1}f_{7/2}]\pi + [i_{13/2}^{-1}g]\nu)$. Definitions of shells: $g \equiv g_{9/2}$, $r \equiv i_{11/2}d_{3/2}d_{5/2}g_{7/2}s_{1/2}$. The experimental data are plotted with a black continuous line. For ^{214,216}Pb the range of measured $B(E2)$ values is indicated with a shaded area.

observed $8^+ \rightarrow 6^+$ transitions and also for the other transitions. Finally, the sign of the quadrupole moments is now again coherent with case A. Therefore, the inclusion of the p-h excitations from the core in a nonstandard way, i.e., with an explicit coupling equivalent to consider effective three-body interactions, goes in the direction of improving the experimental data. In this regard, it is important to notice that discrepancies between calculated and experimental $B(E2)$ values of seniority isomers in the first $g_{9/2}$ shell have been found for protons in ^{98}Cd [26] and neutrons in ^{72}Ni [27], and they have been attributed to proton-dripline and seniority-mixing effects, respectively. Instead, the results of the present work suggest that those discrepancies may have the same origin and therefore come from the neglect of effective three-body forces.

In summary, state-of-the-art experimental techniques have allowed us to measure the $B(E2)$ reduced transition probabilities of the isomeric states in neutron-rich lead isotopes, which have shown quantitative discrepancies with the theoretical predictions. The inclusion of effective three-body forces, studied via the dressing of the bare wave function with p-h excitations, substantially improves the agreement with experimental data. This work is thus a first hint of the importance of properly treating the effective many-body terms, and it will serve as both a stimulus and benchmark for future shell-model calculations, demanding a full perturbative analysis of the renormalization process all over the nuclide chart.

We acknowledge Morten Hjorth-Jensen for providing the two-body matrix elements from the CD-BONN interaction. The work of the GSI accelerator staff is acknowledged. A. G., M. D. and E. F. acknowledge the support of INFN, Italy and MICINN, Spain, through the AIC10-D-000568 action. A. G. has been partially supported by MICINN, Spain and the Generalitat Valenciana, Spain, under Grants No. FPA2008-06419 and No. PROMETEO/2010/101. The support of the UK STFC and AWE plc, and of the DFG(EXC 153) is also acknowledged.

*andrea.gottardo@lnl.infn.it

[1] E. Caurier, F. Nowacki, A. Poves, and A. P. Zuker, Rev. Mod. Phys. **77**, 427 (2005).
[2] A. J. Daley, J. M. Taylor, S. Diehl, M. Baranov, and P. Zoller, Phys. Rev. Lett. **102**, 040402 (2009).
[3] G. Bertsch, Phys. Rev. Lett. **21**, 1694 (1968).
[4] A. Poves, E. Pasquini, and A. P. Zuker, Phys. Lett. **82B**, 319 (1979).
[5] A. P. Zuker, Phys. Rev. Lett. **90**, 042502 (2003).
[6] T. Otsuka, T. Suzuki, J. D. Holt, A. Schwenk, and Y. Akaishi, Phys. Rev. Lett. **105**, 032501 (2010).
[7] R. B. Wiringa and S. C. Pieper, Phys. Rev. Lett. **89**, 182501 (2002).
[8] A. Banu *et al.*, Phys. Rev. C **72**, 061305(R) (2005).
[9] C. Vaman *et al.*, Phys. Rev. Lett. **99**, 162501 (2007).
[10] H. Geissel *et al.*, Nucl. Instrum. Methods Phys. Res., Sect. B **70**, 286 (1992).
[11] S. Pietri *et al.*, Nucl. Instrum. Methods Phys. Res., Sect. B **261**, 1079 (2007).
[12] P. H. Regan *et al.*, Nucl. Phys. **A787**, 491 (2007).
[13] R. Kumar *et al.*, Nucl. Instrum. Methods Phys. Res., Sect. A **598**, 754 (2009).
[14] P. H. Regan *et al.*, Int. J. Mod. Phys. E **17**, 8 (2008).
[15] M. Pfützner *et al.*, Phys. Lett. B **444**, 32 (1998).
[16] C. Ellegaard, P. D. Barnes, and E. R. Flynn, Nucl. Phys. **A170**, 209 (1971).
[17] A. de Sahlit and I. Talmi, *Nuclear Shell Theory* (Dover Publications, New York, 1963).
[18] R. F. Casten, *Nuclear Structure from a Simple Perspective* (Oxford University Press, New York, 2001).
[19] E. Caurier and F. Nowacki, Acta Phys. Pol. B **30**, 705 (1999).
[20] E. Caurier, G. Martínez-Pinedo, F. Nowacki, A. Poves, J. Retamosa, and A. Zuker, Phys. Rev. C **59**, 2033 (1999).
[21] E. K. Warburton and B. A. Brown, Phys. Rev. C **43**, 602 (1991).
[22] I. Hamamoto, Phys. Rep. **10**, 63 (1974).
[23] D. G. Kovar, N. Stein, and C. K. Bockelman, Nucl. Phys. **A231**, 266 (1974).
[24] R. Machleidt, Phys. Rev. C **63**, 024001 (2001).
[25] M. Dufour and A. P. Zuker, Phys. Rev. C **54**, 1641 (1996).
[26] M. Górska *et al.*, Phys. Rev. Lett. **79**, 2415 (1997).
[27] M. Sawicka *et al.*, Phys. Rev. C **68**, 044304 (2003).